

Coherent anti-Stokes Raman scattering in PrF₃

Karl P. Traar*

Institut für Allgemeine Elektrotechnik und Elektronik, Abteilung für Quantenelektronik und Lasertechnik, Technische Universität, A-1040 Wien, Austria

(Received 25 August 1986)

I report the observation of Raman resonances due to the ${}^3H_4 \rightarrow {}^3F_2$ transition in Pr³⁺ ions by coherent anti-Stokes Raman scattering. The very weak resonances could only be measured in PrF₃ under cryogenic conditions (2 K). The ratio $C = |\chi^{(3)R}/\chi^{(3)NR}|_{\max}$ did not exceed 0.5 for the most intense resonances. This value is in good agreement with realistic estimations for the resonant contribution $\chi^{(3)R}$ of the Pr³⁺ ions and $\chi^{(3)NR}$ due to the host crystal.

I. INTRODUCTION

Transparent rare-earth (RE) compounds have played an important role in the development of many new high-resolution techniques in laser spectroscopy. They provided sharp optical features as well as the high atomic density of condensed matter. The high intensity of light available from laser sources has made possible the field of multiphoton spectroscopy. Again rare-earth crystals have played an important historical role: the first observation of two-photon absorption (TPA) occurred in a crystal containing Eu²⁺.¹ The theory of rare-earth two-photon processes (TPA and electronic Raman scattering) was developed by Axe² as early as 1964. In TPA spectroscopy only a few studies have explored the sharp spectral lines of rare-earth ions in the seventies.³⁻⁵ Not until recently did the studies of Bloembergen and co-workers bring new experimental and theoretical results in TPA of rare-earth crystals^{6,7} and lead to some modification of the standard theory of Axe.⁸ Electronic Raman scattering (ERS) has been more popular,⁹⁻¹¹ primarily used to determine the positions and symmetries of the electronic lines in the far infrared. Despite some recent exceptions, other nonlinear optical processes such as stimulated Raman scattering and four-wave mixing are lacking.¹²⁻¹⁴ TPA is usually studied via the anti-Stokes luminescence they induce after two-photon (TP) excitation. In addition to a direct TP excitation two-step excitations may also lead to anti-Stokes luminescence^{15,16} making the interpretation of the spectra quite cumbersome. Fluorescence quenching in concentrated materials and nonradiative decay may prohibit the

detection of TPA. The detection of electronic Raman resonances in conventional Raman scattering may often be hindered by fluorescence light. TPA or Raman resonant four-wave mixing is not influenced by these effects and thus can be advantageous.¹⁷ In the case of Raman resonances the most popular four-wave mixing technique is known as coherent anti-Stokes Raman scattering (CARS).

The intensity of a coherent wave mixing signal scales like the square of a sum of a nondispersive, nonresonant susceptibility $\chi^{(3)NR}$ and a dispersive, resonant $\chi^{(3)R}$,¹⁸ which contains useful spectroscopic information. Therefore the critical parameter for a four-wave mixing technique to be advantageous over conventional methods is the ratio C of the maximum resonant to the nonresonant susceptibility ($C = |\chi_{\max}^{(3)R}/\chi^{(3)NR}|$). To obtain useful spectroscopic data, C should be as large as possible. It is the purpose of this paper to determine this ratio in a rare-earth compound with electronic Raman resonances and to demonstrate the possibilities of an improvement of the conventional "amplitude CARS" by a background suppression method.^{19,20} I decided to investigate the Pr³⁺ ion because of its large cross section²¹ and hence large $\chi^{(3)R}$. In order to keep $\chi^{(3)NR}$ as small as possible I selected a trifluoride crystal, which is transparent until about 200 nm.

II. THEORY

The four-wave mixing process can be described by a third-order nonlinear susceptibility $\chi^{(3)}$, which in the case of Lorentzian Raman-active lines may be written²²

$$\begin{aligned} \chi_{ijkl}^{(3)}(-\omega_{AS}; \omega_L, \omega_L, -\omega_S) &= \chi_{ijkl}^{(3)NR} + \chi_{ijkl}^{(3)R} \\ &= \chi_{ijkl}^{(3)NR} + \frac{NL}{(24\hbar)} \sum_f \frac{\tilde{\alpha}_{ij,f}(\omega_{AS}, -\omega_L) \alpha_{kl,f}(\omega_L, -\omega_S) + \tilde{\alpha}_{ik,f}(\omega_{AS}, -\omega_L) \alpha_{jl,f}(\omega_L, -\omega_S)}{\Omega_{fg} - (\omega_L - \omega_S)}, \end{aligned} \quad (1)$$

where i, j, k, l refer to the polarization directions of the anti-Stokes beam ω_{AS} , the pump beam ω_L , and the Stokes beam ω_S , respectively, $\chi^{(3)NR}$ is a nondispersive part which stems from the crystal, α_{ij} and $\tilde{\alpha}_{ij}$ are polarizability matrix elements given by

$$\begin{aligned} \tilde{\alpha}_{ij,f}(\omega, -\omega_x) &= -\frac{e^2}{\hbar} \sum_a \frac{\mu_{ga}^{(i)} \mu_{af}^{(j)}}{\Omega_{ag} - \omega} + \frac{\mu_{ga}^{(j)} \mu_{af}^{(i)}}{\Omega_{ag}^* + \omega_x}, \\ \alpha_{ij,f}(\omega_x, \omega_y) &= -\frac{e^2}{\hbar} \sum_a \frac{\mu_{fa}^{(i)} \mu_{ag}^{(j)}}{\Omega_{ag} - \omega_y} + \frac{\mu_{fa}^{(j)} \mu_{ag}^{(i)}}{\Omega_{ag} - \omega_x}. \end{aligned} \quad (2)$$

If the pump beam ω_L is off electronic resonance we have $\tilde{\alpha}_{ij} = \alpha_{ij}^*$. $\mu_{ga}^{(i)}$ represents the i th component of the dipole matrix $\langle g | \boldsymbol{\mu} | a \rangle$. In (2) $\Omega_{fg} = \omega_{fg} - i\Gamma_{fg}$ and ω_{fg} and Γ_{fg} are the associated resonance frequencies and widths of the level f , N is the number of resonant scatterers per unit volume, L is a local-field correction factor. With $\Delta_f = \omega_{fg} - (\omega_L - \omega_S)/\Gamma_{fg}$, $\tilde{\chi}_f^R = |\chi_f^R(\Delta_f=0)|$, and $C = \tilde{\chi}_f^R/\chi^{NR}$ the anti-Stokes intensity of the signal normalized to the off-resonance intensity may be written²³ as

$$I_S/I_S^{NR} = \left| \frac{\chi^{(3)NR} + \chi^{(3)R}}{\chi^{(3)NR}} \right|^2 = 1 + 2C \frac{\Delta}{\Delta^2 + 1} + C^2 \frac{1}{\Delta^2 + 1}. \quad (3)$$

The detectability of a two-photon resonant signal depends on the magnitude of C and is limited to values of $C \simeq 5 \times 10^{-2}$. An improvement of this described amplitude CARS (Ref. 20) can be obtained by suppression of the nonresonant background by suitable arrangement of the polarization directions of the pump beams ω_L and ω_S . If the polarization direction of the ω_L beam is the x direction and the polarization direction of the ω_S beam makes

$$(\hat{\boldsymbol{\epsilon}}_S \cdot \mathbf{D} \hat{\boldsymbol{\epsilon}}_L \cdot \mathbf{D}) = -6 \sum_l F(l)^2 \sum_t (2l+1)^{1/2} \begin{Bmatrix} 1 & 3 & l \\ 3 & 1 & t \end{Bmatrix} (\underline{\boldsymbol{\epsilon}}_S^{(1)} \underline{\boldsymbol{\epsilon}}_L^{(1)})^{(t)} \cdot \underline{\mathbf{U}}^{(t)}, \quad (6)$$

$$F(l) = (-1)^l [7(2l+1)/3]^{1/2} \begin{Bmatrix} 3 & 1 & l \\ 0 & 0 & 0 \end{Bmatrix} \langle 4f | r | nl \rangle.$$

This result is due to Downer⁷ (see also Ref. 8) and is equivalent to the result of Axe.² In (6) $\hat{\boldsymbol{\epsilon}}_S$ and $\hat{\boldsymbol{\epsilon}}_L$ are the polarization unit vectors of the Stokes and pump beam, respectively, \mathbf{D} is the sum of the radius vectors \mathbf{r}_j for all electrons j , $\underline{\boldsymbol{\epsilon}}_S^{(1)}$ and $\underline{\boldsymbol{\epsilon}}_L^{(1)}$ are spherical unit vectors for the Stokes and pump beam and $\underline{\mathbf{U}}^{(t)}$ is the unit tensor operator of rank t . The scalar part ($t=0$) vanishes in this approximation,²⁵ the antisymmetric ($t=1$) and anisotropic ($t=2$) part can be calculated with the help of Refs. 26 and 27. For intermediate coupled wave functions the matrix elements of $\underline{\mathbf{U}}^{(2)}$ are available from Ref. 28. The contribution of the anisotropic part often dominates over the antisymmetric part and we may take only the first one into account.

Higher-order contributions to lanthanide two-photon processes have been taken into account to explain recent experimental results in Gd^{3+} TPA.^{5,6} I have calculated the third-order contribution with spin-orbit coupling in the intermediate states $4f5d$ of Pr^{3+} for the transitions ${}^3H_4 \rightarrow {}^3H_4, {}^3H_5, {}^3F_2$ and found that it is smaller than 1% of the second-order contribution and hence can be neglected.²⁹ A rough estimate for the average contribution to the resonant susceptibility $\tilde{\chi}_{xxxx}^R$ of PrF_3 at 2 K from the ground state to the excited state Stark level can be made by calculating the product $[(2J+1)(2J'+1)]^{-1} \times$ (line strength) for x polarizations. $2J+1$ and $2J'+1$ are the ground- and excited-state Stark-level multiplicities, respectively. For PrF_3 and $\Gamma/2\pi c \simeq 1.5 \text{ cm}^{-1}$ I estimate $\tilde{\chi}_{xxxx}^{(3)R} \simeq 4 \times 10^{-16}$ esu for the ${}^3H_4 \rightarrow {}^3F_2$ transition. Smith

an angle δ to the x direction, then the nonlinear polarization due to $\chi^{(3)NR}$ oscillates in a plane with an angle²⁴

$$\alpha = \arctan \left[\left(\frac{\chi_{xyyx}^{NR}}{\chi_{xxxx}^{NR}} \right) \tan \delta \right] \quad (4)$$

to the xz plane. Nulling the nonresonant field with a polarization analyzer, the intensity at the detector becomes²⁰

$$I_D = K \left| \frac{(\rho_R - \rho_{NR}) \sin \delta \cos \delta}{(\cos^2 \delta + \rho_{NR} \sin^2 \delta)^{1.2}} \right|^2 \times |\chi_{xxxx}^R|^2 I(\omega_L)^2 I(\omega_S), \quad (5)$$

where K is a constant and $\rho_{NR} = \chi_{xyyx}^{NR}/\chi_{xxxx}^{NR}$ and $\rho_R = \chi_{xyyx}^R/\chi_{xxxx}^R$. I note that this technique works only when the symmetries of the resonant and nonresonant susceptibility differ ($\rho_{NR} \neq \rho_R$). The polarizability matrix elements in (2) are usually calculated within the closure approximation and under assumption of constant energy denominators for the intermediate states. To lowest order in perturbation theory one finds the following useful expression:

estimated $\chi_{xxxx}^{(3)NR} \simeq 7 \times 10^{-16}$ esu for LaF_3 by comparing his CARS results in LaF_3 and benzene.²⁰ Because of the similar structure of LaF_3 and PrF_3 I may assume $\chi^{(3)NR}$ for PrF_3 to be of the same order of magnitude and may expect the parameter C to be of order 1 for the transition ${}^3H_4 \rightarrow {}^3F_2$ in PrF_3 . The intensities and their polarization dependences for the individual Stark components are difficult to predict quantitatively, because of the lack of knowledge of the wave functions. In PrF_3 the rare-earth (RE) ions occupy six homologous sites per unit cell (D_{3d}^4) of site symmetry C_2 and have totally symmetric transforming ground states (A of C_2).^{30,31} With a ground state $|g\rangle$ of symmetry Γ_g , and a final state $|f\rangle$ of symmetry Γ_f , the excitation symmetry Γ_x is that of the operator $|f\rangle\langle g|$ given by $\Gamma_x = \Gamma_f \times \Gamma_g^*$.³² For a final state with symmetry A (B) we get in our case an excitation symmetry of the A (B) type. Neglecting the scalar and antisymmetric contributions the scattering tensor in a local coordinate system XYZ of a RE ion (the C_2 axis is the Z axis) may have the following nonvanishing components:

$$\alpha_{XX} = a, \quad \alpha_{YY} = b, \\ \alpha_{ZZ} = -(\alpha_{XX} + \alpha_{YY}), \quad \alpha_{XY} = \alpha_{YX} = d$$

for A -type excitation;

$$\alpha_{XZ} = \alpha_{ZX} = g, \quad \alpha_{YZ} = \alpha_{ZY} = h$$

for B -type excitation. The local susceptibility components

TABLE I. Nonvanishing Raman resonant susceptibility components. $\chi_{ijkl}^{(3)R}(\omega_{AS}; \omega_L, \omega_S, -\omega_S)$ of PrF₃ for local *A* and *B* excitations of the Pr³⁺ ion ($A_f = NL / [(24\hbar\Gamma_{fg})(\Delta_f - i)]$).

A-type	$\chi_{xxxx}^{(3)R} = \chi_{yyyy}^{(3)R} = A_f [(\frac{9}{2})a^2 + 6ab + 6b^2]$
	$\chi_{zzzz}^{(3)R} = A_f 12a^2$
	$\chi_{xxyy}^{(3)R} = \chi_{yyxx}^{(3)R} = \chi_{xyxy}^{(3)R} = \chi_{xyyx}^{(3)R} = A_f (\frac{3}{2})a^2$
	$\chi_{xyyx}^{(3)R} = \chi_{yxxy}^{(3)R} = A_f [(\frac{3}{2})a^2 + 6ab + 6b^2]$
	$\chi_{zxzx}^{(3)R} = \chi_{zyzy}^{(3)R} = \chi_{yzyz}^{(3)R} = \chi_{zxzx}^{(3)R} = \chi_{zyzy}^{(3)R} = \chi_{zxzx}^{(3)R} = \chi_{zyzy}^{(3)R} = \chi_{zyzy}^{(3)R} = \chi_{zxzx}^{(3)R} = A_f 6e^2$
B-type	$\chi_{xxxx}^{(3)R} = \chi_{yyyy}^{(3)R} = \chi_{xxyy}^{(3)R} = \chi_{xyxy}^{(3)R} = \chi_{yxxy}^{(3)R} = A_f 6h^2$
	$\chi_{xxyy}^{(3)R} = \chi_{yyxx}^{(3)R} = -A_f 6h^2$
	$\chi_{zzzz}^{(3)R} = 0$
	$\chi_{zxzx}^{(3)R} = \chi_{zyzy}^{(3)R} = \chi_{yzyz}^{(3)R} = \chi_{zxzx}^{(3)R} = \chi_{zyzy}^{(3)R} = \chi_{zxzx}^{(3)R} = \chi_{zyzy}^{(3)R} = A_f 6g^2$

may be determined with formula (2) and may be transformed to the laboratory frame (*z* axis = *C*₃ axis of the factor group *D*_{3d}). The resulting resonant susceptibility components are listed in Table I. For RE in most crystal lattices the size of interaction between neighboring ions is so small that Davydov splitting is not resolved and hence the resonant susceptibility of all unresolved excitons has the same polarization dependence as the composite susceptibility of the corresponding single-ion excitations on all the equivalent sites in the primitive cell.³² For local *A*- (*B*-) type excitation the resonant susceptibility has the same polarization dependence as the susceptibility resulting from *A*_{1g} + *E*_g (*A*_{2g} + *E*_g) modes.

III. EXPERIMENTAL DETAILS

A PrF₃ crystal with size 7 × 7 × 7 mm³ was obtained by Optovac Inc. and immersed into a liquid helium bath at 2 K. The *c* axis was aligned parallel to the pump beam ω_L . This beam was part of the output from a 10-Hz repetition rate doubled Quanta Ray DCR1 Nd-YAG laser (YAG denotes yttrium aluminum garnet). This laser also pumped a Spectra Physics PDL1 giving a tunable output between 720 and 750 nm. The energy difference between the dye laser and the doubled YAG laser photons lies in the range of the ³F₂ crystal-field levels. The duration of the pump beams was approximately 8 nsec and the energy per pulse was 0.1 mJ. Both beams were focused together with a *f*₁ = 10 cm lens into the crystal with an angle α between ω_L and ω_S to achieve phasematching. In the range of interest a maximum output was obtained for $\alpha \cong 5.7^\circ$. Before each scan phasematching was optimized for each subrange. The anti-Stokes output was made parallel by a *f*₂ = 10 cm lens, sent through a double monochromator and detected by a RCA 1P28 photomultiplier (PM). The PM signal was integrated and normalized to the intensity of the dye laser beam ω_S , which was scanned between 720 to 750 nm, and displayed on a chart recorder. A computer controlled the simultaneous tuning of the dye laser and the monochromator. For the background suppressing (BS) CARS spectra, the polarization direction of the ω_S beam was rotated with respect to the ω_L beam by 71.5° (Ref. 33) and an analyzing system (polarization rotator plus analyzer) was set in the ω_{AS} beam to suppress the

off-resonance signal. A Babinet Soleil compensator was used to compensate the slight ellipticity of the off-resonance signal, which is due to birefringence in the optical components.

IV. EXPERIMENTAL RESULTS AND DISCUSSION

Within the range of the ³F₂ crystal field levels I found two electronic Raman resonances [see Figs. 1(a), 1(b), 2(a), and 2(b)], which I term *R*₁ and *R*₂ in this paper. Resonancelike structures were found near 5200 cm⁻¹, and, if true resonances, may stem from two lines (*R*₃ and *R*₄

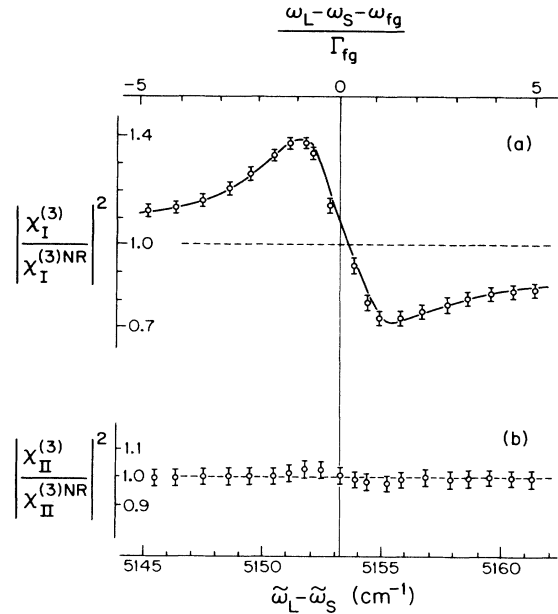


FIG. 1. Intensity of the coherent anti-Stokes Raman wave generated in PrF₃ at 2 K for $\tilde{\omega}_L - \tilde{\omega}_S = (\omega_L - \omega_S) / 2\pi c$ near 5150 cm⁻¹. Small circles with error bars indicate measured points, while the solid line is a fitted curve with the parameters listed in Table II. The scale is normalized to a value of off resonance. The abbreviations $\chi_I^{(3)} = \chi_{xxxx}^{(3)}$ (a) and $\chi_{II}^{(3)} = \chi_{xyyx}^{(3)}$ (b) are used.

TABLE II. Experimentally determined positions, widths, and C values of PrF_3 .

$ijkl$	$\omega/2\pi c$ (cm^{-1})	$\Gamma/2\pi c$ (cm^{-1})	$C = \chi_{ijkl}^{(3)R} / \chi_{ijkl}^{(3)NR}$
xxxx	5153.2 ± 0.5	1.65	0.33 ± 0.03
	5191 ± 2		< 0.05
	5214 ± 2		< 0.05
	5300.6 ± 0.5		0.14 ± 0.03
xyyx	5153.2 ± 0.5	3.2	< 0.03
	5191.0 ± 2		< 0.05
	5194 ± 2		< 0.05
	5300.6 ± 0.5		0.43 ± 0.03

line). I have fitted my data only for the most intense lines. Table II summarizes the results and the estimated range of positions and C values for the possible resonances near 5200 cm^{-1} . In order to improve the sensitivity I tried to resolve the resonancelike structures by background-suppression CARS (BS CARS). This spectrum shows clearly the resonance line R_1 (see Fig. 3), but still cannot resolve the weak lines R_3 and R_4 found in the amplitude CARS. This may be due to a near coincidence of ρ_R and ρ_{NR} and/or imperfections in nulling the non-resonant background. As seen in Fig. 3 the background due to off resonance ellipticity is rather large. This is mainly due to the birefringence of the cryostat windows and cannot be compensated enough.

The experimentally determined C values of our CARS signal lie within the range of my rough estimates for the theoretical value for this parameter. Although an exact determination of the symmetry of the lines would require

a complete determination of all polarization dependences (I would need to measure susceptibility components with z indices) I may determine some consequences of the data. Since the line R_1 was detected only in an xxxx spectrum, it is very likely to be of A_{1g} symmetry. The disappearance of the E_g part of this line may be accidental or due to interaction of the RE ions. I could not find an E_g line in the vicinity of the R_1 line. Thus the first assumption sounds more realistic and the R_1 line should be a consequence of a local A -type excitation. This agrees with the determination due to fluorescence measurements.^{31,34} I note, however, that the measured line is shifted 3 cm^{-1} to higher energies compared with the position reported in Ref. 35.

Due to Kleinmann symmetry, I can assume $\chi_{xxxx}^{NR} = 3\chi_{xyyx}^{NR}$ and hence it follows from Table II that $\chi_{xxxx}^R = \chi_{xyyx}^R$ for the R_2 line. This should be a conse-

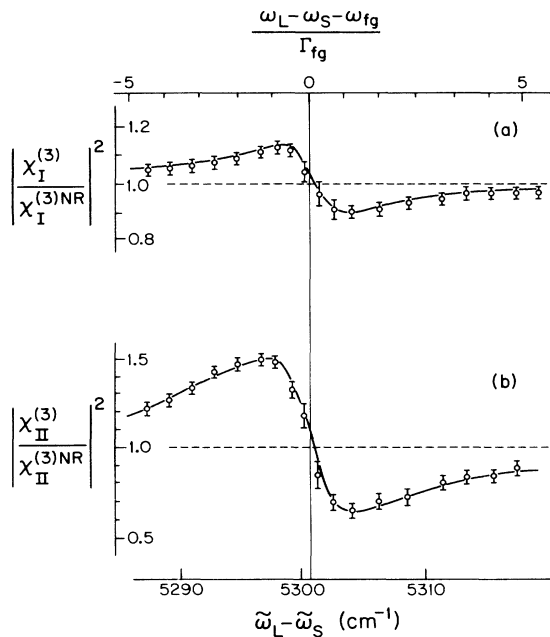


FIG. 2. Intensity of the coherent anti-Stokes wave with $\tilde{\omega}_L - \tilde{\omega}_S$ near 5300 cm^{-1} . Symbols and abbreviations as in Fig. 1.

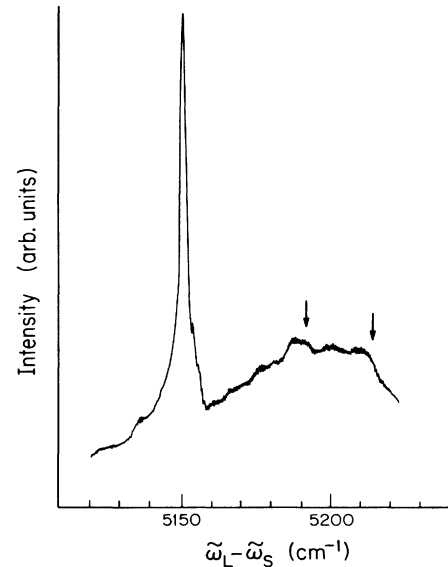


FIG. 3. Intensity of the coherent anti-Stokes wave in BS CARS [see formula (5) in the text]. The nonresonant background field was nulled at 5050 cm^{-1} . The R_1 line found in amplitude CARS [see Fig. 1(a)] is easily detected, R_3 and R_4 lines cannot be resolved unambiguously. Arrows indicate positions of lines measured by ${}^3P_0 \rightarrow {}^3F_2$ fluorescence (after Ref. 34).

quence of a local B -type excitation and contradicts the determination of Ref. 34. The position of this level is shifted 5 cm^{-1} to higher energies compared to the position determined by fluorescence. Within the errors of my measurement the positions of our R_3 and R_4 line, if true resonances, correspond well to Dahl's fluorescence data.

The reason for this discrepancy is not understood to date. It would be interesting to determine the symmetry of these lines by a conventional Raman scattering experiment.

V. CONCLUSION

I have measured a two-photon resonant four-wave mixing signal in a trivalent rare-earth compound by amplitude CARS and tried to test a BS CARS for the first time in such a system. I have chosen a crystal which I expected to have a small nonresonant susceptibility and a rare-earth ion transition with large cross section. Even under

these circumstances the resonances due to different crystal-field levels are very weak. The resonances were only observable in a fully concentrated material at 2 K. The BS CARS did not allow me to detect the very weak resonances of the amplitude CARS unambiguous. The reasons may be the limitation of this technique due to birefringence in the optics and a depolarization ratio $\rho_R \cong \frac{1}{3}$.

ACKNOWLEDGMENTS

I would like to thank Professor A. J. Schmidt for stimulation of this study and thank Professor P. Weinberger, Prof. G. Marovsky, Dr. M. Dahl, and Dr. G. Reider for the helpful discussions. The technical assistance of the latter is also gratefully acknowledged. This work was supported by the Fonds zur Förderung der wissenschaftlichen Forschung under Grant No. P5283.

*Present address: Dept. of Physics and Astronomy, University of Georgia, Athens, GA 30602.

¹W. Kaiser and C. G. B. Garrett, *Phys. Rev. Lett.* **7**, 229 (1961).

²J. D. Axe, *Phys. Rev.* **136**, A42 (1964).

³P. A. Apanasevich, R. I. Gintoft, V. S. Korolkov, A. G. Makhanev, and A. G. Skripko, *Phys. Status Solidi B* **58**, 745 (1973).

⁴U. Fritzler and G. Schaack, *J. Phys. C* **9**, 123 (1976).

⁵A. G. Makhanev and G. A. Skripko, *Phys. Status Solidi A* **53**, 243 (1979).

⁶M. C. Downer and A. Bivas, *Phys. Rev. B* **28**, 3677 (1983); M. C. Downer, C. D. Cordero-Montalvo, and H. Crosswhite, *ibid.* **28**, 4931 (1983); M. Dagenois, M. Downer, R. Neumann, and N. Bloembergen, *Phys. Rev. Lett.* **46**, 561 (1981); M. Downer, A. Bivas, and N. Bloembergen, *Opt. Commun.* **41**, 335 (1982).

⁷M. C. Downer, Ph.D. thesis, Harvard University, 1983 (unpublished).

⁸R. R. Judd and D. R. Pooler, *J. Phys. C* **15**, 591 (1982).

⁹J. A. Konigstein and O. S. Mortensen, *Phys. Rev.* **168**, 75 (1968).

¹⁰J. A. Konigstein and G. Schaack, *Phys. Rev. B* **2**, 1242 (1970).

¹¹K. Leiteritz and G. Schaack, *J. Raman Spectrosc.* **10**, 36 (1981).

¹²M. L. Shand, *J. Appl. Phys.* **52**, 1470 (1981).

¹³D. A. Ender, M. S. Otteson, R. L. Cone, and M. B. Ritter, *Opt. Lett.* **7**, 611 (1982).

¹⁴K. Tyminski, R. C. Powell, and W. K. Zwicker, *Phys. Rev. B* **29**, 6074 (1984).

¹⁵P. A. Apanasevich, R. I. Gintoft, and A. G. Makhanev, *Zh. Prikl. Spektrosk.* **16**, 443 (1972).

¹⁶D. Narayana Rao, Jagdish Prasad, and Paras N. Prasad, *Phys. Rev. B* **28**, 20 (1983).

¹⁷P. A. Apanasevich, L. A. Dzheguryan, and A. G. Makhanev,

Zh. Prikl. Spektrosk. **38**, 296 (1983).

¹⁸M. D. Levenson and J. J. Song, in *Coherent Raman Spectroscopy*, in Vol. 21 of *Topics in Current Physics* (Academic, New York, 1980), p. 293.

¹⁹A. Akhmanov and N. I. Koroteev, *Usp. Fiz. Nauk* **123**, 405 (1977) [*Sov. Phys. Usp.* **20**, 899 (1977)].

²⁰R. W. Smith, Ph.D. thesis, Berkeley University (1980).

²¹A. Kiel and S. P. S. Porto, *J. Mol. Spectrosc.* **32**, 458 (1969).

²²H. Lotem, R. T. Lynch, Jr., and N. Bloembergen, *Phys. Rev. A* **14**, 1748 (1976).

²³I. Itzkan and D. A. Leonard, *Appl. Phys. Lett.* **26**, 106 (1975).

²⁴J. L. Oudar, R. W. Smith, and Y. R. Shen, *Appl. Phys. Lett.* **34**, 758 (1979).

²⁵R. D. Peacock, *Struct. Bonding* (Berlin) **22**, 83 (1975).

²⁶M. Rotenberg, R. Bivins, N. Metropolis, and J. K. Wooten, Jr., *The 3-j and 6-j Symbols* (MIT, Cambridge, Mass., 1959).

²⁷C. W. Nielson and G. F. Koster, *Spectroscopic Coefficients for the p^N, d^N, f^N Configurations* (MIT, Cambridge, Mass., 1964).

²⁸W. T. Carnall, H. Crosswhite, and H. M. Crosswhite, Argonne National Laboratory Report, 1977 (unpublished).

²⁹K. P. Traar, Ph.D. thesis, Technische Universität Wien, 1986 (unpublished).

³⁰M. Dahl and G. Schaack, *Phys. Rev. Lett.* **56**, 232 (1986).

³¹M. Dahl, Ph.D. thesis, Julius Maximilians Universität Würzburg, 1985 (unpublished).

³²W. Hayes and R. Loudon, *Scattering of Light by Crystals* (Wiley, New York, 1978).

³³N. I. Koroteev, M. Endemann, and R. L. Byer, *Phys. Rev. Lett.* **43**, 398 (1979).

³⁴M. Dahl and G. Schaack, *Z. Phys. B* **56**, 279 (1984).

³⁵The experimental value of the lowest Stark level of 3F_2 was tabulated erroneously in Ref. 34. The correct position due to fluorescence measurements should be 5150 cm^{-1} . This was reported by M. Dahl in a private communication.